Distribution of scaled height in one-dimensional competitive growth profiles

T. A. de Assis,[1,*] C. P. de Castro,[1] F. de Brito Mota,[1] C. M. C. de Castilho,[1,2] and R. F. S. Andrade[1]

[1]*Instituto de Física, Universidade Federal da Bahia, Campus Universitário da Federação, 40170-115 Salvador, BA, Brazil*

[2]*Instituto Nacional de Ciência e Tecnologia em Energia e Ambiente (CIENAM)INCT-EA, Universidade Federal da Bahia, Campus Universitário da Federação, 40270-280 Salvador, BA, Brazil**

(Received 12 June 2012; revised manuscript received 3 September 2012; published 15 November 2012)

This work investigates the scaled height distribution, $\rho(q)$, of irregular profiles that are grown based on two sets of local rules: those of the restricted solid on solid (RSOS) and ballistic deposition (BD) models. At each time step, these rules are respectively chosen with probability p and $r = 1 - p$. Large-scale Monte Carlo simulations indicate that the system behaves differently in three succeeding intervals of values of p: $I_B \approx [0,0.75)$, $I_T \approx (0.75,0.9)$, and $I_R \approx (0.9,1.0]$. In I_B, the ballistic character prevails: the growth velocity v_∞ decreases with p in a linear way, and similar behavior is found for $\Gamma_\infty(p)$, the amplitude of the $t^{1/3}$-fluctuations, which is measured from the second-order height cumulant. The distribution of scaled height fluctuations follows the Gaussian orthogonal ensemble (GOE) Tracy-Widom (TW) distribution with resolution roughly close to 10^{-4}. The skewness and kurtosis of the computed distribution coincide with those for TW distribution. Similar results are observed in the interval I_R, with prevalent RSOS features. In this case, the skewness become negative. In the transition interval I_T, the system goes smoothly from one regime to the other: the height distribution becomes apparently Gaussian, which motivates us to identify this phenomenon as a transition from Kardar-Parisi-Zhang (KPZ) behavior to Edwards-Wilkinson (EW) behavior back to KPZ behavior.

DOI: 10.1103/PhysRevE.86.051607 PACS number(s): 81.15.Aa, 73.90.+f, 05.45.Df, 61.43.Hv

I. INTRODUCTION

In recent years there have been remarkable and successful efforts to control, measure, and understand the growth of disordered surfaces on 1D and 2D substrates using experimental, analytical, and numerical approaches [1–9]. In addition to being an intriguing scientific challenge, this problem has attracted considerable technological interest. Many properties of specifically devised materials depend on rough surfaces that are formed under nonequilibrium conditions.

From the theoretical point of view, the investigation of surface growth has been significantly dominated by successive analytical and numerical proposals for solving the Kardar-Parisi-Zhang (KPZ) equation [10],

$$\partial_t h(x,t) = \mu_0 + \mu\triangle h + \frac{\lambda}{2}(\nabla h)^2 + \eta(x,t), \qquad (1)$$

where μ_0 corresponds to a constant driving force and $\eta(x,t)$ is white Gaussian noise. This equation contains a nonlinear term that, despite being simple, accounts for a considerable number of experimental results that cannot be described by the linear Edwards-Wilkinson (EW) equation [3,11], which is recuperated by setting $\lambda = 0$ in Eq. (1).

The first efforts toward solving the KPZ equation were based on a scaling theory that leads to the scaling exponents associated with the self-affine profiles. For correlated systems such as this one, the interface width (Ω) should follow the Family-Vicsek scaling assumptions [3]:

$$\Omega(L,t) \sim t^\beta g(Lt^{-1/z}), \qquad (2)$$

where g is a scale function and β and $z = \alpha/\beta$ correspond to the growth and dynamic exponents, respectively, while α is the roughness exponent. Furthermore, for length scales $L \ll \widetilde{L} \sim t^{1/z}$, Ω follows the power law $\Omega(L) \sim L^\alpha$ and, for the case in which $L \gg \widetilde{L}$, $\Omega(t) \sim t^\beta$.

Research was subsequently directed toward evaluating the probability density functions (pdf) of the scaled height fluctuations. The seminal work in this direction was identifying that an exact pdf solution for the height distribution of the KPZ solution can be expressed in terms of Tracy-Widom (TW) distributions [4–6]. For different geometric conditions, they assume different forms that, in this case, obey the statistics of the Gaussian orthogonal ensemble (GOE) or the Gaussian unitary ensemble (GUE). Recent numerical results [8,9] hint to the universality of the GOE and GUE distributions in discrete growth models on flat and circular one-dimensional substrates, respectively. This relationship supports the experimental results obtained for the growth of liquid crystals on substrates with initial flat or curved interfaces [6]. The numerical, experimental, and analytical results build strong evidences for a robust universality class of systems far from equilibrium based on evidences that go beyond the scaling law exponents.

The purpose of this work is to present new results for the stochastic growth of irregular 1D profiles considering two different sets of local rules, namely the ballistic deposition (BD) and the restricted solid-on-solid (RSOS) models. We identify the conditions where the scaled height fluctuation distribution of the competitive model belongs to some of the TW universality classes. We performed careful numerical simulations that allow, in addition to direct comparison with the TW distributions, the evaluation of the linear growth rate velocity (v_∞), the amplitude of the $t^{1/3}$-fluctuations (Γ_∞), and the skewness (S) and the kurtosis (K) of the resulting distributions. For most situations, the resulting profile fits well into the TW framework. However, we demonstrate that it is

*thiagoaa@ufba.br

possible to fine-tune two individual processes that individually lead to TW distributions in such a way that any fingerprint of the two nonlinear growth models is removed. In this range, all the aforementioned measures become typical of the the linear growth model, which motivates this phenomenon to be identified as a KPZ-EW-KPZ transition.

The remainder of this work is organized as follows: Sec. II introduces the competitive growth model based on two sets of deposition rules. The results are discussed in Sec. III, which is divided into three subsections: in the first one, we discuss the numerical procedures used to obtain reliable values of the growth exponents, υ_∞ and Γ_∞. Then, we present a detailed characterization of the height fluctuation distributions, ρ, in two intervals (I_B and I_R), where the characteristic features are those of the BD and RSOS single models. Finally, the third subsection is devoted to the analysis of the transition interval, I_T, where the typical features of the linear models appear. Section IV closes the paper with our concluding remarks.

II. COMPETITIVE GROWTH MODEL

There are many models that describe the growth processes of interfaces and surfaces, which are defined by local deposition rules. Such systems have different physical properties that are reflected in the scaling exponents, in the scaled height fluctuation distribution, etc. Nevertheless, models with quite distinct local rules may share intrinsic properties. This is the case, for instance, of the RSOS and BD models. Despite being quite different, theoretical considerations of the continuous limits of these models indicate that both of them are described by the same Eq. (1) [12], although their values of λ have opposite signs. For both systems, the reported values for the roughness and growth exponents agree with the values of $\alpha_{\rm KPZ} = 1/2$ and $\beta_{\rm KPZ} = 1/3$ [3].

Let us consider a competitive version of the RSOS and BD models mentioned above. We begin with a square lattice that has discrete values of x, $j \in [1,L]$ and $h \geqslant 0$. At the initial time $t = 0$, the lattice is empty. The profile is grown by vertically dropping mass elements over the different columns, j, such that, at each discrete value of the time t, the profile is described by the function $h = h(j,t)$, which identifies the largest value of h in column j that is occupied by a mass element. During each deposition event, a particle is released from a position, (j,h') $j \in [1,L], h' > h_{\max}(t)$, that is randomly chosen above the surface, and it falls vertically onto the growing substrate. Here, $h_{\max}(t)$ represents the largest value of h that is occupied by a mass element at time t. The falling particle will follow the RSOS deposition rule with probability p, and the BD rule with probability $r = 1 - p$. For the first case, the falling particle will adhere to site j if the condition $|\Delta h(j,t)| = |h(j,t) - h(j \pm 1,t)| \leqslant M$ is satisfied, where M is the parameter that controls the roughness of the rough interface. Hereafter, we always consider $M = 1$.

In the BD case, the released particle falls vertically until it touches the surface and irreversibly adheres to the first site that has an occupied nearest neighbor. Therefore, this feature considers the possibility of lateral growth. The BD model generates a bulk material that has porosity and a positive nonlinear parameter, because the growth velocity is greater than the deposition rate.

III. RESULTS

A. Scaling properties

We performed Monte Carlo simulations with $L \in [10^2, 10^6]$ considering finite-size effects to define the onset of asymptotic scaling. Finite-size effects stay at the ground of numerical discrepancies that are often observed between the obtained values of the growth exponents and $\alpha_{\rm KPZ}$ or $\beta_{\rm KPZ}$. Furthermore, there is an inherent difficulty in calculating β, which is related to the lack of a precise criterion to establish the limits of the growth region [where $\Omega(t) \sim t^\beta$] for each system with size L. This question becomes of utmost importance for evaluating the height fluctuation distribution of finite systems because it is globally associated with a Gaussian function when t increases beyond the scaling region. Indeed, for $t \gg L^z$, it is hypothesized that the distribution of the height fluctuations becomes time independent and converges to a Gaussian curve $\rho(\delta h) \propto \exp[-(\delta h)^2/\kappa L]$, where κ is a nonuniversal constant [13] and $\delta h = h - \langle h \rangle$.

To clarify the limits of the growth region, we conducted a detailed analysis of the evaluation of β. Figure 1 presents a detailed study of the dependence of β on L in the case of $p = 0$. We can clearly observe differences between the value of β_L and $\beta_{\rm KPZ}$ as a consequence of finite-size effects. If we assume that β_L depends on L according to $\beta_L = \beta_0(1 - L^{-\gamma})$, our results lead to $\beta_0 = 0.338 \pm 0.003$ and $\gamma = 0.250 \pm 0.009$ when $p = 0$ (BD), which is in excellent agreement with previous numerical results [14,15]. In the inset of the same figure, we indicate the growth region that was used to calculate β_L. To determine this region, we adopted the following procedure: (i) identify the interval in which the curve of $\log_{10}[\Omega(t)] \times \log_{10}[t]$ is apparently linear; (ii) fit the points in this region with a high-degree polynomial function; (iii) identify the interval where the derivative of $\log_{10}[\Omega(t)]$ as a function of $\log_{10}[t]$ is nearly constant; and (iv) evaluate the value of β as the slope of the best linear fit in the identified interval.

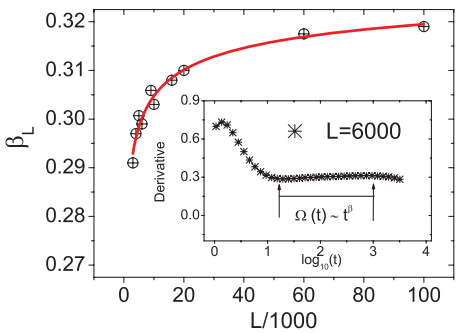

FIG. 1. (Color online) Dependence of β_L on L for $p = 0$. Finite size effects cause a discrepancy between β_L and $\beta_{\rm KPZ}$. The solid red line indicates the ansatz function $\beta_L = \beta_0(1 - L^{-\gamma})$, with best fitting values $\beta_0 = 0.338 \pm 0.003$ and $\gamma = 0.250 \pm 0.009$. The inset shows the derivative of the polynomial function that best fits the numerical values of $\log_{10}[\Omega(t)]$ as a function of $\log_{10}[t]$ for $L = 6\,000$. It is used to estimate the growth interval $[\Omega(t) \sim t^\beta]$ for the calculation of β_L.

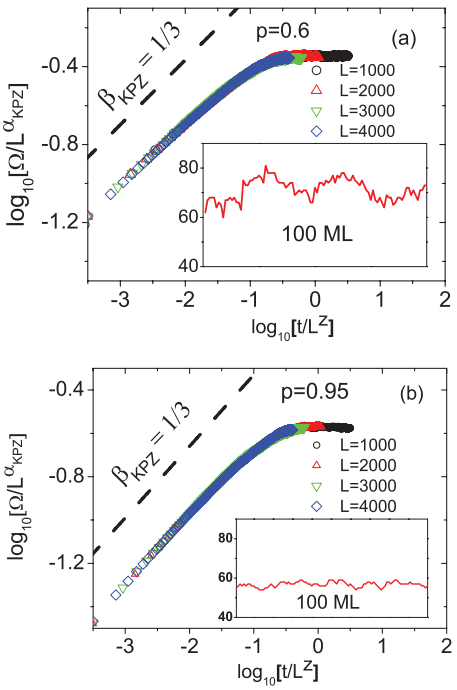

FIG. 2. (Color online) Dependence of the interface width Ω with respect to t using Family-Vicsek scaled variables. $1+1$ dimensional KPZ values of α and z are used for the RSOS + BD competitive model: (a) $p = 0.6$; (b) $p = 0.95$. The dashed lines indicate the KPZ growth exponent $\beta_{\rm KPZ} = 1/3$. In the corresponding insets, the solid red (gray) line indicates the profile after deposition of 100 monolayers.

Before discussing the height fluctuations, it is important to recall that, for a profile $h(j,t)$ growing on a finite substrate, the long time limit, $1 \ll t \ll L^z$ [16], obeys the equation

$$h(j,t) = t\left[\upsilon_\infty \pm \left(\frac{\Gamma_\infty}{t^2}\right)^{1/3} q\right], \qquad (3)$$

where υ_∞ represents the interface growth velocity and Γ_∞ is related to the parameter λ and depends on the growth model. q represents a time-independent random variable used for the purpose of comparing our numerical estimates with the analytical solution for the KPZ equation. The analytical solution for the KPZ equation is such that the distribution $\rho(q)$ is a pertinent TW distribution. Therefore, the comparison of our results with those for the KPZ equation is conducted by comparing the distribution $\rho(q)$ resulting from the numerical simulations with the GOE distribution, $\rho_{\rm TW}(q) = \rho(\chi)$.

In Fig. 2, we present numerical results for $\Omega(t)$ as a function of t for $p = 0.6$ and $p = 0.95$. In both panels, it is possible to realize that, by considering Eq. (2) together with the values of $\beta_{\rm KPZ}$ and $\alpha_{\rm KPZ}$, we obtain a data collapse for the results with different values of L. This collapse is verified for both the growth region and for the flat part of the curve that represents the correlated growth. The typical features of the curves shown in Fig. 1 for $p = 0$ are also reproduced when we consider the values of p used in Fig. 2. This result reflects the fact that the competitive growth model presents the self-affinity described by the KPZ critical exponents for large intervals of p. The validity of this result, which was rigorously obtained in the hydrodynamic limit for both the pure BD ($p = 0$) and RSOS ($p = 1$) models, is preserved when the two processes are competitive in the intervals $I_B \approx [0,0.75)$ and $I_R \approx [0.9,1]$. In the transition interval $I_T \approx (0.75,0.90)$, β deviates from $\beta_{\rm KPZ}$. A previous study of competitive growth models involving the BD and RSOS rules [17] reported the value of $\beta \approx 0.27$ when $p \sim 0.83$, which remains close to that of the linear model ($\beta_{\rm EW} = 1/4$) [3,11]. Our simulations indicate that the $p = 0.83$ competitive model becomes even closer to the EW model. When $L = 10^5$, the procedure illustrated in Fig. 1 leads to $\beta \approx 0.265$.

B. Height distribution: Nonlinear regime

Let us present results that, together with height distribution fluctuations in the growth region, go beyond the exponent evaluation and allow for a detailed characterization of the three intervals: I_B, I_T, and I_R. We first estimate the parameter υ_∞, which is related to λ in Eq. (1). For a rough interface whose dynamics are governed by the KPZ equation, the average velocity in a given scale ℓ, not considering the drift velocity due to external forces, is given by $\upsilon = \lambda/\ell \int_0^\ell dx\sqrt{1+(\nabla h)^2}$. Assuming $(\nabla h)^2 \ll 1$, $\upsilon \approx \lambda + \lambda/2\ell \int_0^\ell dx(\nabla h)^2$. If there is an average slope $m = \langle \nabla h \rangle$ within an interval of length ℓ of the interface, the result indicates that the velocity of the interface within that interval is approximately given by: $\upsilon(m) \approx \lambda + (\lambda/2)m^2$. Thus, $\upsilon(m)$ is the slope-dependent velocity that should be observed in the coarse-grained scale ℓ. Then, $\lambda = \upsilon(m = 0) = \upsilon_\infty$ [18,19].

In the insets of Fig. 2, the morphology of the resulting exposed interface (red line) after the deposition of 100 monolayers is shown. These results clearly indicate that υ_∞, which was determined by the rate of temporal variation of the mean height of the interface $\langle h \rangle$, is a function of p. According to Eq. (3), we obtain that $d\langle h \rangle/dt \approx \upsilon_\infty + ct^{-2/3}$, where c is a constant [18]. In Fig. 3(a), we show the dependence of the growth velocity υ_∞ as a function of the parameter p. The values for the limit situations, $p = 0$ and $p = 1$, are in good agreement with quite recent results [9]. Our results indicate that the interface growth velocity monotonically decreases with p, and we can clearly identify different decreasing regimes. The first one is characterized by a linear behavior when $p \in [0,0.75]$. For $p \in I_T$, the behavior of υ_∞ is more complex. In fact, the KPZ scaling assumption [Eq. (3)] breaks down. This result is illustrated in the inset of Fig. 3(a). In this inset, we can follow the procedure for estimating the velocity when considering $p = 0.6$. For $p = 0.8$, the linear dependence between $d\langle h \rangle/dt$ and $t^{-2/3}$ [Eq. (3)] is not valid. This is the reason why the estimation of $\upsilon_\infty(p = 0.8)$, which roughly corresponds to the center of I_T, is subject to large fluctuations. Finally, the values of υ_∞ can be computed again for $p = 0.9$ and 1.0. The decreasing straight line linking these two points is considerably less tilted than the one that approximates the discrete points in the interval [0,0.75].

We also evaluate the amplitude of the $t^{1/3}$ fluctuations from the second-order height cumulant $\Omega^2(t) \simeq (\Gamma t)^{2/3}\langle \chi^2 \rangle_c$. For large values of time, this quantity provides information about the most likely value and confidence interval for estimating the parameter Γ_∞, which depends on how $\langle \chi^2 \rangle_c$ is normalized. We consider $\langle \chi^2 \rangle_c$ as the variance of $\rho(\chi)$ ($\sim$0.63805) [9,20]. Figure 3(b) demonstrates how the parameter Γ_∞ varies with

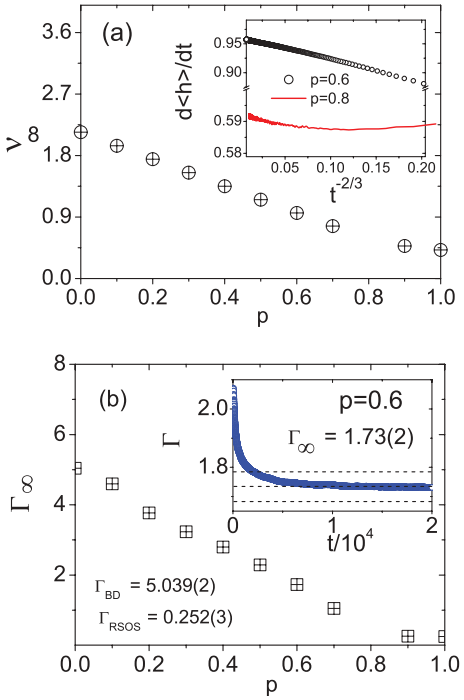

FIG. 3. (Color online) (a) The interface growth velocity $v_\infty(p)$ as a function of p for the competitive RSOS + BD model. In the limit situations, $v_\infty(p=0) = 2.142(7)$ and $v_\infty(p=1) = 0.4191(4)$. In the inset, the procedure for estimating the velocity $d\langle h\rangle/dt$ for $p = 0.6$. For $p = 0.8$ [solid red (gray) line], Eq. (3) is not valid. (b) The dependence of the parameter Γ_∞ with respect to p, with a change in the derivative $d\Gamma/dp$ in the interval I_T. In the inset, the Γ_∞ estimation procedure for $p = 0.6$ is presented.

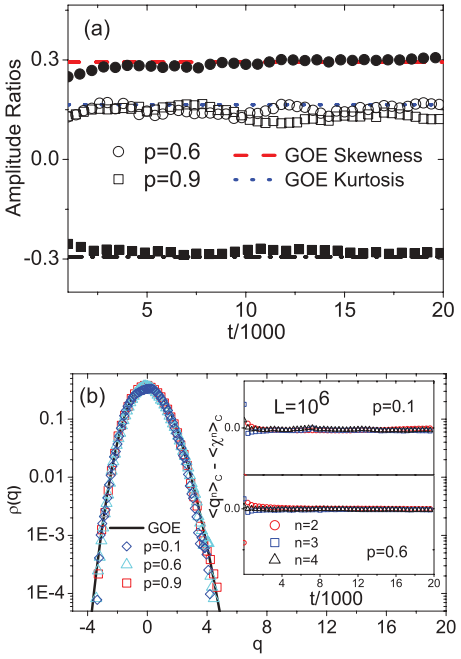

FIG. 4. (Color online) (a) Amplitude ratios (Skewness and kurtosis) of the measured height distribution as a function of time for $p = 0.6$ and $p = 0.9$. The skewness and the kurtosis for $\rho(\chi)$, respectively, $S_{\rm TW} = 0.2935$ and $K_{\rm TW} = 0.1652$, are indicated by the dashed and dotted lines [20]. (b) Distribution of scaled height fluctuation for $p = 0.1$,0.6, and 0.9. The numerical results are compared with GOE distribution, indicated by the solid black line. In the inset, the differences between the cumulants resulting from the simulations $\langle q^n\rangle_c$ and the corresponding GOE TW values $\langle\chi^n\rangle_c$, for $p = 0.1$ and $p = 0.6$.

the probability p. We can then observe a similar transition behavior as that observed for v_∞ when $p \in I_T$, an evidence of an abrupt change in the growth dynamics. In the corresponding inset, we illustrate the procedure adopted for estimating Γ_∞ for $p = 0.6$.

Now we analyze several features of the height distributions that are associated with irregular profiles. With the nth order cumulants (n = 2, 3, and 4) of the local height, $\langle h^n\rangle_c$, we determine $S = \langle h^3\rangle_c/(\langle h^2\rangle_c^{3/2})$ and $K = \langle h^4\rangle_c/(\langle h^2\rangle_c^2)$ [18]. We clearly observe in Fig. 4(a) that, in the growth region, both quantities are nonzero, which suggests that the interface fluctuations are not Gaussian. Furthermore, S agree particularly well with those associated to $\rho(\chi)$ ($S_{\rm TW} = 0.2935$) [20], except in the case where $p = 0.8$. With the exception of this value of p, the values of $v_\infty(p)$ and $\Gamma_\infty(p)$ allow for the calculation of $\rho(q)$, which is the distribution of scaled height fluctuations, where $q \equiv [h - v_\infty(p)t]/[\Gamma_\infty(p)t]^{\beta_{\rm KPZ}}$. In this procedure, we consider the growth interval for each system according to the conditions $1 \ll t \ll L^z$.

Figure 4(b) illustrates the behavior of the height fluctuation distribution. For three distinct values of p within the intervals I_B and I_R, the resulting pdf converges to the GOE distribution (left side). This result is consistent with theoretical results for the KPZ equation and supports our claims that, in these two intervals, the competitive model also falls into the same universality class. In the inset of this figure, we present the nth order cumulants ($\langle q^n\rangle_c$) for the scaled height obtained from our simulations together with those for the GOE TW distributions $\langle\chi^n\rangle_c$. A rapid convergence is observed for $p = 0.1$ and $p = 0.6$.

C. Height distribution: Transition interval

Let us discuss the results of p in the interval I_T. Note that I_T is not symmetrically placed within the [0,1] interval, which indicates that the BD character prevails for a larger range of p values than that of the RSOS. I_T can be divided into two subintervals, $I_{T,1}$ and $I_{T,2}$; in the first one, the system undergoes a KPZ-EW transition, which is reversed in $I_{T,2}$.

First, consider the dependence of S with p. In Fig. 5(a), we observe that when $p \in I_{T,1} \approx (0.75,0.83)$, S is positive but decreases monotonically, departing from $S_{\rm TW}$, until $p \sim 0.83$, when it becomes ≈ 0. Similar behavior is observed for the kurtosis (not shown); it departs from $K_{\rm TW}$ at $p \sim 0.75$, decreases monotonically, and becomes ≈ 0 at $p \sim 0.83$. For $p \in I_{T,2} \approx (0.83,0.90)$, S becomes negative, approaching the limit $-S_{\rm TW}$ as $p \to 0.9$, whereas $K \to K_{\rm TW}$ in this same limit. This result enables a break of the KPZ universality class to be identified in the whole interval I_T. Simultaneously, the EW universality class is only observed for a single point in the interval, where it is reasonable to suppose that the growth phenomenon is essentially linear.

In Fig. 5(b), we show how the asymptotic value of S changes with p. Such dependence can be well represented by sigmoidal

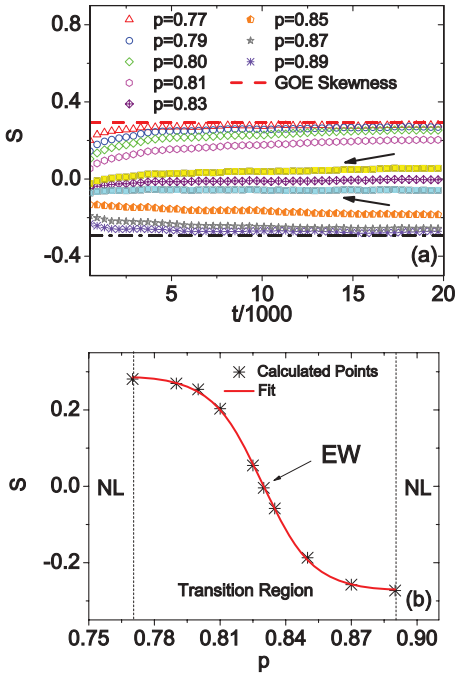

FIG. 5. (Color online) (a) Skewness as a function of the time computed for different probabilities $p \in I_T$. The dashed line correspond to the GOE skewness. The arrows highlight the skewness para $p = 0.83 \pm \epsilon$ com $\epsilon = 0.005$. (b) Skewness as a function of p. The solid line corresponds to sigmoid function [Eq. (4)], with the inflexion point at $p \approx 0.83$ where the skewness is close to zero. The arrow locates the system with EW-like features. NL indicates the nonlinear regime.

curve

$$S(p) = c_1 + \frac{c_2 - c_1}{1 + \exp\left[w(p - p_0)\right]} \tag{4}$$

(obtained $R^2 = 0.999$), where $c_1 \approx 0.27$, $c_2 \approx -0.28$, the inflexion point $p_0 = 0.8293$ coincides with the value previously identified by the simulation ($p \approx 0.83$), and $w \approx 37.4 \times \ln(10)$.

To provide a complete picture of the resulting distributions in I_T, we illustrate in Fig. 6 the depart from the produced distribution with respect to the GOE TW curve for some values of p in this interval. In this figure, we use the scaled $\Omega\rho(\delta h/\Omega)$ function as a function of $h \to (\delta h)/\Omega$ when $p = 0.79$, 0.83, and 0.87. In addition, for the purpose of providing a better comparison of the points when $p \in I_T$, we also draw the inverted TW distribution $\rho(-\chi)$. When $p = 0.79$, the simulation results show a slight deviation from $\rho(\chi)$ in the left tail, with larger than expected contributions at larger values of $\delta h/\Omega$, in contrast with a very good agreement in the right-hand side. This result is in agreement with a positive S, albeit smaller than S_{TW}. For $p = 0.83$, the simulation distribution becomes fairly symmetric, with clear deviations of the asymptotic behavior on both sides of $\rho(\chi)$. Finally, for $p = 0.87$, the distribution should be compared with $\rho(-\chi)$ with a negative S. We again identify a fairly good agreement in the right tail. Nevertheless, the deviations from $\rho(\chi)$ in the left-hand side results from smaller than expected contributions at larger values of $\delta h/\Omega$. This result explains why S is less negative than $-S_{\mathrm{TW}}$.

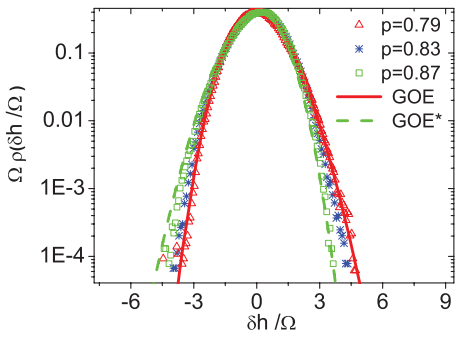

FIG. 6. (Color online) Scaled height $(\delta h)/\Omega$ distributions for $p = 0.79, 0.83$, and 0.87. The solid and dashed lines correspond to $\rho(\chi)$ with positive and negative skewness, respectively.

IV. CONCLUSIONS

In this work, we conducted large-scale Monte Carlo simulations of a competitive growth model based on two different sets of local rules, which individually lead to the same KPZ universality class. The high quality of our results, together with a careful analysis of the scaling regions, permitted essential features of the scaled height distributions to be determined. Our results provide a detailed characterization of the dependence of the average growth rate υ_∞, the fluctuation magnitude Γ_∞, and the height scaled distribution as a function of p. All of these parameters present distinct behaviors in three ranges of p values, which we identified as I_B, I_T, and I_R. The first and the third ones are well described by GOE $\rho(\chi)$, albeit with inverted parity. The detailed investigation of the scaled height distribution in the the transition interval I_T identified how its form changes continuously, which produces changes in the values of S and K. In particular, we described two mechanisms that account for the deviation of the produced distribution with respect to GOE $\rho(\chi)$ when p has just entered and is about to leave I_T.

These results have interesting consequences in constructing experimental devices, because a choice of p can allow us to control irregularities (departs from TW distribution) that can move the TW limits $\chi \to \pm\infty$. Then, by exerting an adequate control in the surface growth process (for example, by direct interference) such that the resulting geometry adequately deviates from the TW distribution in the right asymptotic limit, it is possible to optimize the final produced electronic current density. This fact is being systematically investigated in our group with the purpose of simulating field emitter devices with irregular surfaces. Such deviations from the asymptotic limits of TW distributions may even appear in the promising field of emitter materials (conducting polymers) that are grown on 2D substrates.

In conclusion, the results of this study provide the possibility to analyze the height distributions of a more realistic growth composed of competitive models that establish the limits where the TW distributions can also be observed.

ACKNOWLEDGMENTS

This work has been supported by CNPq (Brazil) by means of researcher grants and through the INCT-SC project, FAPESB (Brazil) under PRONEX 0006/2009 project, and CAPES (Brazil). T.A.d.A. acknowledges Herbert Spohn for providing the Tracy-Widom distributions data.

[1] P. Meakin, Phys. Rep. **235**, 189 (1993).
[2] J. C. Russ, *Fractal Surfaces* (Plenum, New York, 1994).
[3] A. L. Barabasi and H. E. Stanley, *Fractal Concepts in Surface Growth* (Cambridge University Press, Cambridge, 1995).
[4] T. Sasamoto and H. Spohn, Phys. Rev. Lett. **104**, 230602 (2010).
[5] K. A. Takeuchi and M. Sano, Phys. Rev. Lett. **104**, 230601 (2010).
[6] K. A. Takeuchi, M. Sano, T. Sasamoto, and H. Spohn, Sci. Rep. **1**, 34 (2011).
[7] T. Sasamoto and H. Spohn, J. Stat. Mech. (2010) P11013.
[8] S. G. Alves, T. J. Oliveira, and S. C. Ferreira, Europhys. Lett. **96**, 48003 (2011).
[9] T. J. Oliveira, S. C. Ferreira, and S. G. Alves, Phys. Rev. E **85**, 010601 (2012).
[10] M. Kardar, G. Parisi, and Y.-C. Zhang, Phys. Rev. Lett. **56**, 889 (1986).
[11] D. D. Vvedensky, Phys. Rev. E **67**, 025102 (2003).
[12] T. J. Oliveira and F. D. A. Aarao Reis, Phys. Rev. E **76**, 061601 (2007).
[13] T. Halpin-Healy and Y. Zhang, Phys. Rep. **254**, 215 (1995).
[14] F. D. A. Aarao Reis, Phys. Rev. E **63**, 056116 (2001).
[15] B. Farnudi and D. D. Vvedensky, J. Phys.: Conf. Series **286**, 012031 (2011).
[16] S. N. Majumdar, Les Houches **85**, 179 (2007).
[17] T. J. da Silva and J. G. Moreira, Phys. Rev. E **63**, 041601 (2001).
[18] K. A. Takeuchi and M. Sano, J. Stat. Phys. **147**, 853 (2012).
[19] J. Krug, P. Meakin, and T. Halpin-Healy, Phys. Rev. A **45**, 638 (1992).
[20] M. Prahofer and H. Spohn, Phys. Rev. Lett. **84**, 4882 (2000).